
Journal of Computer-Aided Materials Design, **6:** 337–347, 1999.
KLUWER/ESCOM

Hierarchical modeling of C and Si nano-cluster nucleation utilizing quantum and statistical mechanics

GREGORY A. JOHNSON and NASR M. GHONIEM*
Mechanical and Aerospace Engineering Department, University of California at Los Angeles (UCLA), Los Angeles, CA 90095-1597, U.S.A.

Received 1 September 1999; Accepted 21 October 1999

Abstract. A hierarchical, multi-scale computer model for the nucleation of nano-phase materials from the vapor phase is presented. The model utilizes full solutions to quantum mechanics cluster energy equations for sizes up to 10 atoms, and statistical rate theory for larger cluster sizes. Ab initio and semi-empirical quantum mechanics methods are used to investigate the energetics of Si and C clusters. The results of binding energy and most stable configurations show significant differences between C and Si nano-clusters. Atomic cluster size distributions are obtained from reaction rate theory on the basis of collision frequencies in the vapor phase. Cluster reaction rates are determined from the energetics and vibrational modes, as investigated by quantum mechanics for small sizes. The nucleation and further evolution of the cluster size distribution is modeled by solutions to detailed kinetic equations. This multi-scale model is shown to be a useful computer simulation tool, which can be utilized to design experiments on nano-phase materials with minimum adjustable parameters.

Keywords: Carbon, Nano-clusters, Nucleation, Plasma, Quantum chemistry, Silicon, Statistical mechanics

1. Introduction

Nano-clusters are normally manufactured by various techniques including organic precursor-based synthetic chemistry, aqueous colloidal processing, low temperature thermalization of organo-rare-earth clusters, metallo-organic pyrolysis [1], and laser ablation of different materials [2]. All of these synthesis techniques rely upon cluster growth mechanisms, which are controlled by the chemistry of participating species. Chemical techniques are used for producing semiconductor nano-crystals, for example, and are also generally accompanied by the formation of unanticipated byproducts [3]. Furthermore, the chemical sensitivity towards oxidation or reducibility of chemical constituents, plus the necessary care in the choice of anion or cation precursor components, greatly impacts control of nano-crystal production. Chemical reaction rates, or limited availability of suitable chemical precursors, can limit the composition, type and size [4] of nano-particles and nano-particle-based structures that can be obtained. When plasma processing is considered as a route to nano-cluster manufacturing, additional degrees of freedom become available to control nano-particle formation and deposition. Independent control of the ion and neutral densities, the temperature of each species, the kinetic energy of the atom or ion-cluster interactions, the particle deposition energy, and many other parameters, is possible in a plasma environment. The flexibility of this technique allows it to be used for making bulk material, thin films, and coatings. In addition, the ability to produce and sustain a nonequilibrium state to drive the desired plasma chemistry or reaction rates provides many new possibilities for scientists to explore and understand the fabrication

* To whom correspondence should be addressed.

and manipulation of nano-particles. Because of the large number of plasma process variables, however, an accurate model for the evolution of cluster size distribution is needed.

The size of most nano-phase materials is on the order of 100 nm or less, and contains fewer than tens of thousands of atoms. Conventional materials, on the other hand, consist of grains ranging from microns to millimeters, and contain several billion atoms. The small size of the grains and the grain size distribution is what gives nano-phase materials their unique properties, many of which are still under investigation. The key in practical utilization of nano-phase materials is accurate control of the grain size and size distribution, allowing the properties of the material to be tailored for a specific requirement. Theoretical methods for accurately determining the properties of nano-phase materials based on their size distribution are needed to predict properties before the materials are produced.

The primary focus of this paper is to present a model that describes the nucleation, formation, and evolution of the cluster size distribution of nano-phase carbon and silicon within a plasma environment. The objective is to explore methods that enable control of the cluster size distribution, and to eliminate the characteristic tail as a result of competition between nucleation of small size clusters and growth of larger ones. This tail is characteristic of all experimental results to date (See, for example Reference 5). The goal of this research is to develop a detailed model of sufficient accuracy to model and plan relevant experiments. With this model, investigations of the effects of quench rate, pulsed feed mode, and other parameters of interest on the cluster size distribution can be carried out.

2. Cluster nucleation model

Current approaches to modeling the formation of nano-clusters are based on classical nucleation theory. Isolated atoms or molecules combine to form embryos, which are unstable until a critical size is reached. The vapor pressure and surface tension of the material at the temperature and supersaturation of interest determine the critical size for nucleation [6–8]. This approach is not adequate, because the calculated nucleation rate is very sensitive to the exact values of the surface tension and degree of vapor super-saturation. Because the properties of nano-phase materials are fundamentally different from bulk properties, the classical approach of using phenomenological parameters based on bulk properties to describe sequential nucleation and growth of very small particles is questionable. In the following, we present a more fundamental approach to modeling the evolution of nano-clusters in supersaturated vapors, and apply it to the conditions of nucleation within a plasma environment. Quantum mechanics is used to determine cluster energetics for cluster sizes up to 10 atoms. With this information, rate constants are determined. Quantum-Rice-Ramsperger-Kassel (QRRK) theory [9–16], augmented by Transition State Theory [6, 10, 17] and Collision Rate Theory [6, 7, 18], are used to determine the rate constants for clustering reactions. Once this information is in hand, rate equations can be determined, and the evolution of the size distribution studied.

2.1. Quantum chemistry of clusters

The objective of performing quantum mechanical calculations is to determine, with great accuracy, a number of parameters that are needed for further rate constant development. These parameters are cluster binding energy, cluster normal modes of vibration and cluster principal moments of inertia. Determination of cluster energetics requires that Schrödinger's equation for the collection of atoms must be solved with all the associated nuclei and electrons in three

dimensions. For a molecule with N nuclei and n electrons, the time-independent Schrödinger equation is given by [6, 10, 21, 22]:

$$H\Psi = (T_N + T_e + V_{Ne} + V_{NN})\Psi = E_T\Psi \tag{1}$$

where H is the Hamiltonian, and T and V are the kinetic and potential energy operators, respectively. The subscripts N and e refer to nuclear and electronic components, respectively. Exact solutions of the multi-electron, multi-nucleus Schrödinger equation are not available. However, several methods for determining approximate solutions have been developed. Most modern approaches rely on the implementation of the Born–Oppenheimer (BO) approximation. [10, 21, 22]. Because the nuclei are much more massive than the electrons, they are assumed to be stationary. Henceforth the kinetic energy of the nuclei is ignored, allowing separation of the total wave function into a product of the electronic (ψ_{elec}) and nuclear (ψ_{nuc}) wave functions.

The energetics of silicon and carbon clusters of sizes up to 10 atoms has been calculated using the General Atomic and Molecular Electronic Structure System (GAMESS) software package [23]. This was accomplished by utilizing the built-in geometry optimizer that locates relative potential energy minima. Because a given cluster may contain several local minima, numerous initial conditions were tried to ascertain that the final configuration is an absolute minimum. Calculations were performed using both ab initio and semi-empirical methods. In the former, the BO approximation and linear combination of atomic orbitals (LCAO) molecular orbital (MO) theory for each electron in the system are utilized. Semi-empirical methods, on the other hand, are based on neglecting differential overlap (NDO) of inner electrons [31]. Calculations were performed with the two methods for silicon clusters, and with the ab initio method only for carbon clusters. The basis sets (e.g. sets of atomic orbitals) used were the TZV [29] basis set for the ab initio calculations and the PM3 [25] basis set for the semi-empirical calculations. In this manner, the cluster binding energy, configuration, and normal modes of vibration were determined. This information is subsequently used when determining the rate constants used to describe nucleation and clustering.

For small size clusters, binding energies determined from quantum mechanics calculations were directly used in subsequent rate calculations. For larger size clusters, however, the binding energy as a function of cluster size was appropriately extrapolated. The method used was the capillary model, Equation 2. Here $E_{binding}$ is the total cluster binding energy, m is the number of bonds per atom, ϕ is the energy per bond and x is the number of atoms in the cluster. The parameter a is a surface parameter which serves as a proportionality constant for the number of surface atoms per bulk atom, and accounts for the average number of bonds a surface atom is deficient with respect to a bulk atom.

$$E_{binding} = m\phi x(1 - a\, x^{-1/3}) \tag{2}$$

The energy per bond is related to the heat of sublimation at 0 K by:

$$\phi = \frac{\Delta H_{sublimation}}{m} \tag{3}$$

The surface parameter, a, can be determined in the following manner: The cluster surface area is given as:

$$S = 4\pi \left(\frac{3x\Omega}{4\pi}\right)^{2/3} \tag{4}$$

where Ω is the atomic volume given as $\Omega = a_0^3/8$ for the diamond structure and $\Omega = \sqrt{3}/8a_0^2c$ for the graphite structure. Assuming that the surface cleaves on a (111) plane for the diamond structure, or at the basal plane for the graphitic structure, the atomic surface density is $\sigma = 4/(\sqrt{3}a_0^2)$ for both the diamond and the graphite structures. Substituting into Equation 4 gives the number of surface atoms as a function of cluster size:

$$x_s = \frac{4\pi}{\sqrt{3}}\left(\frac{3}{4\pi}\right)^{2/3} x^{2/3} \tag{5}$$

for the diamond structure and

$$x_s = \frac{4\pi}{\sqrt{3}}\left(\frac{3}{4\pi}\right)^{2/3}\left(\sqrt{3}c/a_0\right)^{2/3} x^{2/3} \tag{6}$$

for the graphite structure. For the diamond structure, each surface atom on the (111) plane is deficient half a bond (i.e. $\phi/2$). Inserting this into Equation 5 gives the total surface energy of the cluster:

$$E_{Surface}^{Total} = \frac{4\pi}{\sqrt{3}}\left(\frac{3}{4\pi}\right)^{2/3} \phi/2x^{2/3} \tag{7}$$

Then, by inspection,

$$a_{Si} = \frac{\pi}{\sqrt{3}}\left(\frac{3}{4\pi}\right)^{2/3} \tag{8}$$

where $m = 2$ for the diamond structure that has been utilized in Equation 8. For graphite, the basal planes are bound to each other by dispersion forces which are relatively very weak compared to the chemical covalent bonds between atoms in the basal plane [32]. To a first approximation, and according to the Tersoff empirical potential for carbon [33], the bond energy between basal planes can be assumed to be zero. This sets the surface energy parameter for graphite as equal to zero.

2.2. Cluster reaction rates

As previously mentioned, QRRK theory augmented with Transition State Theory and Collision rate theory is used to determine rate constants. QRRK theory was originally developed to explain unimolecular reactions. Later refinements allow its use for bimolecular reactions. The underlying inherent assumptions are the following:

(1) Each cluster consists of s oscillators, where $s = 3m - 6$($s = 3m - 5$ for linear clusters).
(2) Each oscillator has the same fundamental frequency, ν.
(3) The vibrational energy is quantized.
(4) The critical oscillator (where bonds are broken/formed) must contain at least m quanta, where $m = \epsilon_0/h\nu$, for a reaction to occur.
(5) Clusters gain/lose vibrational energy by collisions with the surrounding bath gas.
(6) Statistical redistribution occurs at each collision; and the concentration of clusters in each energized state (containing sufficient vibrational energy to react) is maintained at steady state.

Using silicon as an example, the dissociation mechanism is given as:

$$\begin{aligned} Si_{m+n} + M &\xrightarrow{k_1} Si^*_{m+n} + M \\ Si^*_{m+n} + M &\xrightarrow{k_2} Si_{m+n} + M \\ Si^*_{m+n} &\xrightarrow{k_3} Si_m + Si_n \end{aligned} \tag{9}$$

where the first reaction is the rate at which clusters of size $m + n$ are energized to state j; the second reaction is the rate at which these energized clusters are knocked out of state j to a different state; and the third reaction is the rate at which these energized clusters dissociate into clusters of size m and size n. The distribution of vibrational quanta in a cluster is given as [13, 15]:

$$P_j = \frac{(j = s-1)!}{j!(s-1)!} e^{-j\beta h\nu}(1 - e^{-\beta h\nu})^s \tag{10}$$

where j is the number of quanta, s is the number of vibrational modes, $\beta = 1/kT$, h is Planck's constant and ν is the vibrational frequency. The collision rate constant, k_2, at which clusters in vibrational state j are knocked out of this state is given as [18]:

$$k_2 : \sigma\sqrt{8kT/\pi\nu} \tag{11}$$

where σ is the collision cross-section, k is Boltzmann's constant, and μ is the reduced mass of the collision pair. The rate constant, k_1, at which clusters are knocked into vibrational state j is [13]:

$$k_1 = k_2 P_j \tag{12}$$

The rate constant, k_3, at which energized clusters in vibrational state j dissociate is [13, 15]:

$$k_2(j) = A\frac{j!(j-m+s-1)!}{(j-m)!(j+s-1)!} \tag{13}$$

where it has been noted that k_3 is a function of j. Applying the steady state approximation to the excited clusters in vibrational state j gives:

$$k_1[Si_{m+n}][M] = k_2[Si^*_{m+n}][M] + [Si^*_{m+n}] \tag{14}$$

which upon rearrangement and making use of Equation 7 gives:

$$[Si^*_{m+n} = \frac{P_j[Si_{m+n}]}{1 + k_3/k_2[M]} \tag{15}$$

Now the rate of dissociation is $k_3(j)[Si^*_{m+n}]$. Inserting Equation 10 and summing over all energized states, one obtains:

$$k_{diss} = \sum_{j=m}^{\infty} \frac{k_3(j)P_j}{1 + k_3(j)/k_2[M]} \tag{16}$$

Using Equations 10, 11 and 13 and substituting $p = j - m$ into Equation 16 gives the final result [13]:

$$k_{diss} = Ae^{-\varepsilon_0/kT}(1 - e^{-\beta h\nu})^s \sum_{p=0}^{\infty} \frac{\dfrac{(p+s-1)!}{p!(s-1)!}e^{-p\beta h\nu}}{1 + \dfrac{A\dfrac{(p+m)!(p+s-1)!}{p!(p+m+s-1)!}}{\sigma\sqrt{8kT/\pi\mu}[M]}} \tag{17}$$

At high pressures (i.e. large values of $[M]$) Equation 17 becomes [13, 15]:

$$k_{diss} = Ae^{-\varepsilon_0/kT} \tag{18}$$

By constraining the maximum rate constant to that predicted by Transition State Theory [17], the parameter A can be determined to be:

$$A = \left(\frac{kT}{h}\right)\frac{q^{\ddagger}_{m+n}}{q_{m+n}} \tag{19}$$

where $q^{\ddagger}_{m+n}$ is the partition function of the activated complex (e.g. Transition State) and q_{m+n} is the partition function of the cluster. The mechanism for recombination is given as:

$$\begin{aligned} Si_m + Si_n &\xrightarrow{k_4} Si^*_{m+n} \\ Si^*_{m+n} &\xrightarrow{k_3} Si_m + Si_n \\ Si^*_{m+n} + M &\xrightarrow{k_2} Si_{m+n} + M \end{aligned} \tag{20}$$

where the first reaction is the rate of recombination of size m and n clusters to form an energized cluster of size $m + n$ in energized state j. The second reaction is the rate at which energized clusters of size $m + n$ decompose into clusters of size m and n. The last reaction is the rate at which these energized clusters knocked into a different state. By similar arguments used to develop the dissociation rate constant and by applying the principle of detailed balance [26], the recombination rate constant can be shown to be:

$$k_{rec} = A'(1 - e^{-\beta h\nu})^s \sum_{p=0}^{\infty} \frac{\dfrac{(p+s-1)!}{p!(s-1)!}e^{-p\beta h\nu}}{1 + \dfrac{A\dfrac{(p+m)!(p+s-1)!}{p!(p+m+s-1)!}}{\sigma\sqrt{8kT/\pi\mu}[M]}} \tag{21}$$

where now:

$$A' = \left(\frac{kT}{h}\right)\frac{q^{\ddagger}_{m+n}}{q_m q_n} \tag{22}$$

The next step is to calculate the rate constants to be used in the coupled set of ordinary differential equations. For cluster sizes of 10 atoms and less, the information obtained from the ab initio calculations was used to determine the rate constants. The average frequency was determined by using the Einstein model for the heat capacity of a solid, as follows:

$$s\left(\frac{h\bar{\nu}}{kT}\right)^2\left[\frac{e^{h\bar{\nu}/kT}}{\left(e^{h\bar{\nu}/kT}-1\right)^2}\right] = \sum_{j=1}^{s}\left(\frac{h\nu_j}{kT}\right)^2\left[\frac{e^{h\nu_j/kT}}{\left(e^{h\nu_j/kT}-1\right)^2}\right] \tag{23}$$

For larger size clusters, the information required to determine the rate constants was extrapolated from the ab initio calculations or inferred from other physical data. For example, the binding energy was extrapolated using the capillary model previously mentioned. The principal moments of inertia, required for computing the rotational partition function, was determined by assuming a spherical shape and using the density of the bulk solid. The average oscillator frequency was determined by again using the Einstein model for the heat capacity

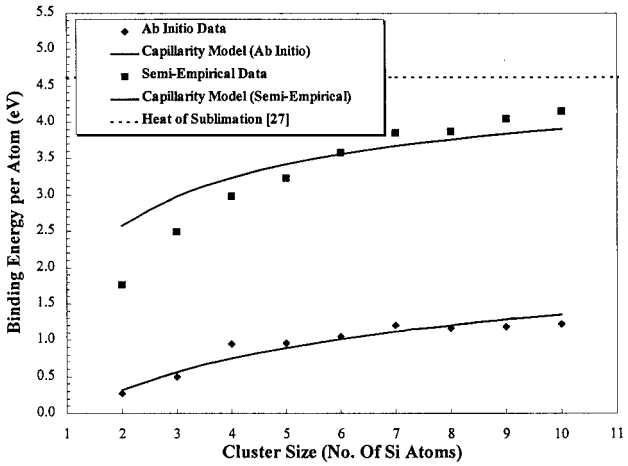

Figure 1. Dependence of the silicon cluster binding energy on its size.

of a solid, but this time finding the Einstein frequency which agreed well with published heat capacity data [28].

2.3. Rate equations for cluster evolution

Now that the rate constants are available, the time-dependent nature of nucleation and clustering can be studied. The time-dependent cluster equation is given as:

$$\begin{aligned} dC_i/dt \; &= 1/2 \sum_{j=1}^{i-1} [K_{rec}(j, i-j) C_j C_{i-j} - 2^{\delta_{j,i-j}} K_{diss}(j, i-j) C_i \\ &+ \sum_{j=1}^{n-i} [2^{\delta_{i,j}} K_{diss}(i, j) C_{i+j} - K_{rec}(i, j) C_i C_j] + S_i \end{aligned} \tag{24}$$

where the first term is the recombination of clusters of size j and $i - j$ to form clusters of size i. The second term is the dissociation of clusters of size i into clusters of size j and $i - j$. The third term if for the dissociation of clusters of size $i + j$ into cluster of size i and j. The fourth term is for the recombination of clusters of size i and j into clusters of size $i + j$. And the last term is a source term which is usually the rate of monomer introduction for $i = 1$ and zero for cluster sizes greater than 1. Equation 24 is a coupled set of stiff, initial value, ordinary differential equations. Solutions of this set of differential equations gives the time-dependent nature of the cluster size distribution. This set of equations is solved using the DVODE software package [29]. DVODE employs a multi-step predictor–corrector technique for solving stiff initial value problems.

3. Results

Figures 1 and 2 show the binding energy per atom for silicon and carbon clusters, respectively, as a function of cluster size for both the ab initio and the semi-empirical model (for silicon only). The symbols are calculated binding energies, while the smooth curves are the binding energies based on the capillary model with best-fit coefficients. The crystalline structure for

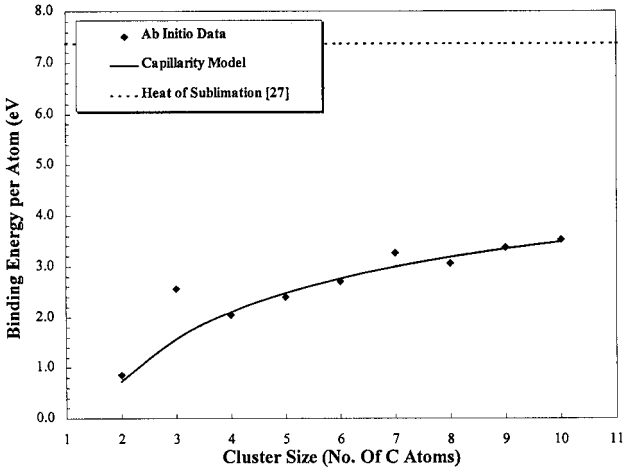

Figure 2. Dependence of the carbon cluster binding energy on its size.

bulk silicon is the diamond structure. Each atom within the bulk of the structure has four nearest neighbors (i.e. each bulk atom is bonded to four other atoms). Therefore, the number of bonds per atom is $m = 2$ for this structure. Likewise, the crystalline structure for bulk carbon (i.e. graphite) is the hexagonal closed pack. Each atom within the bulk of this structure has three nearest neighbors in the basal plane. Thus, for carbon, $m = 1.5$. In order to fit the small cluster data yet approach the bulk crystal heat-of-formation and surface energy for large size clusters, the capillary model, Equation 2 is modified. For silicon, one can observe that the bond angles are highly strained with respect to the bulk crystalline structure (see Fig. 3). Henceforth, it is expected that the average bond energy for small clusters will be reduced. Using this argument, a modified capillary model for silicon is

$$E_{binding} = m\phi(1 - x^{-1/4})x(1 - a\,x^{1/3}) \tag{25}$$

where the power-law term connects small cluster data to bulk properties. For carbon, however, the capillary model worked well without any modifications, but the surface parameter is non-zero. This is not too surprising because the assumption of zero surface energy is a rough approximation in the first place. The reason that the capillary model does not need modification for carbon clusters can be inferred from examining small-size cluster configurations in Fig. 3. It is readily apparent that now the bonds are not strained. Thus the bond energy does not change with cluster size. The difficulty in using the heuristic form of the capillary model just presented for silicon is that it is not based on physical phenomena. It is very useful, nevertheless, because it allows simple determination of the rate constants, as will be discussed later. A heat of sublimation of 4.619 eV for silicon and 7.373 eV for carbon at 0 K [27] was used to determine bond energies. For the semi-empirical model, the bond energy, ϕ, had to be fit to the data yielding binding energies greater than the heat of sublimation for larger size clusters. This is due to the nature of the semi-empirical calculations, where the lack in rigor is augmented with empirical constants. It is plausible that these empirical constants may be adjusted to give better agreement with the ab initio calculations. By determining the cluster binding energy in this manner, the binding energy per atom matches the calculated data while approaching the bulk crystalline heat of sublimation and surface energy for infinite cluster size.

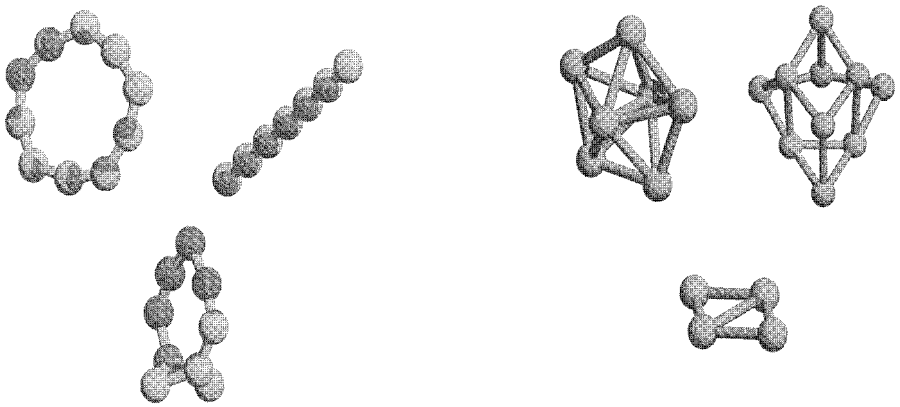

Figure 3. Typical carbon (left) and silicon (right) nano-cluster configurations.

Additionally, cluster configurations were determined for clusters containing up to 10 atoms. Figure 3 shows a sample of computed configurations for carbon and silicon clusters, respectively. It is interesting to note that while Si clusters tend to form diamond-like, compact configurations, C clusters favor the formation of linear and ring-like chains. Although the bond distances differ somewhat, in general, the semi-empirical model predicts the same cluster geometry as the ab initio model.

To illustrate the evolution of cluster size distributions, we solve the system of rate equations, given by Equation 24, up to 300 equations for Si clusters, which are formed by the condensation of Si monomers in argon plasma. The initial monomer concentration is assumed to be 2×10^{21} atoms/cm^3, while the time step is set initially to 1 ms. Monomers are introduced into a plasma nozzle [5] at high temperature, and then the temperature is suddenly decreased as a result of expansion through the nozzle exit. The present calculations are for isothermal conditions at 1100 K. It is observed that the evolution kinetics of small-size clusters (e.g. up to 10 atoms) are extremely fast, and that by 1 ms, their concentrations reach their equilibrium values. However, clustering kinetics of larger-size agglomerates are much slower, and hence the growth of these sizes is over much longer time periods, as can be observed from Fig. 4. Similar calculations [5], with a much more simplified set of equations, indicate that cluster growth occurs near the nozzle exit, while a monotonically decreasing size distribution is obtained at entrance locations, which is consistent with the isothermal conditions of the current investigation.

4. Summary and conclusions

The present method of investigating the nucleation and growth of nano-clusters in plasma environments is very promising. Since cluster energetics are based on ab initio quantum mechanics methods, the predicted properties are highly accurate. The nucleation of larger size clusters can then be studied by statistical mechanics methods, where the rates of cluster interactions are calibrated by the quantum mechanics results for small sizes. The configurations of carbon nano-clusters are markedly different from those of silicon. The calculations indicate that ring and rod nano-clusters of C can be manufactured in plasma processes, while Si nano-clusters tend very quickly to the diamond bulk configuration. Computer simulations of the experimental conditions for clustering within an expanding nozzle, performed at the

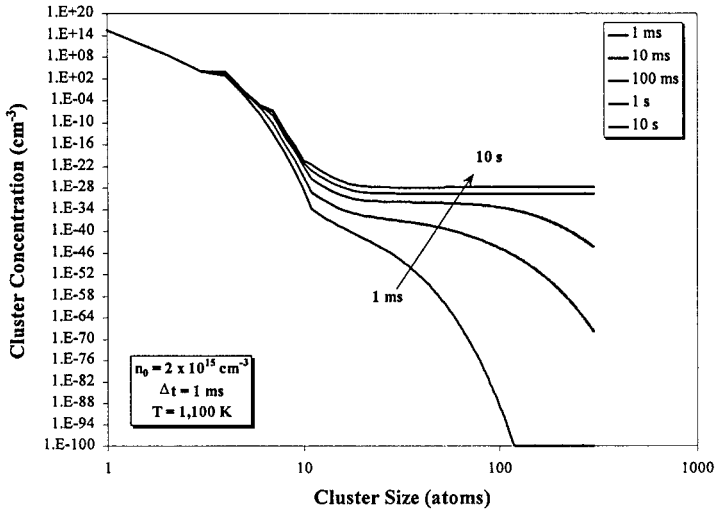

Figure 4. Evolution of Si cluster size distribution from an initial monomer concentration at 1100 K.

University of Minnesota [35], indicate that the evolution of the cluster size distribution is very rapid, and that nucleation is determined by the quench conditions at the nozzle exit. Future work will aim at utilizing the present model to design experiments, which would yield nano-cluster size distributions with desired characteristics (e.g. tight distributions, with diminishing concentrations of large sizes).

References

1. Schwab, S.T., Paul, P.P. and Pan, Y.M., Mater. Sci. Eng., AA204 (1995) 197.
2. Yamamoto, T. and Mazumder, J., Nano-struct. Materials, 7 (1996) 305.
3. Huber, C.A., In Goldstein, A.N. (Ed.) Handbook of Nanophase Materials, Marcel Dekker Inc., New York, NY, 1997, pp. 317–337.
4. Norris, D.J., Sacra, A., Murray, C.B. and Bawendi, M.G., Phys. Rev. Lett., E 72 (1994) 2612.
5. Rao, N. et al., Plasma Chem. Plasma Processing, 15 (1995) 581.
6. Atkins, P.W., Physical Chemistry, 2nd ed., W.H. Freeman and Co., New York, NY, 1982.
7. Seinfeld, J.H. and Pandis, S.N., Atmospheric Chemistry and Physics; From Air Pollution to Climate Change, John Wiley & Sons, New York, NY, 1998.
8. Stucky, G.D., Naval Res. Rev., 3 (1991) 28.
9. Robinson, P.J. and Holbrook, K.A., Unimolecular Reactions, John Wiley & Sons, New York, NY, 1972.
10. Senkan, S.M., Adv. Chem. Eng., 18 (1992) 95.
11. Westmoreland, P.R. et al., AIChE J., 32 (1986) 1971.
12. Dean, A.M. and Westmoreland, P.R., Int. J. Chem. Kinetics, 19 (1987) 207.
13. Kassel, L.S., The Kinetics of Homogeneous Gas Reactions, The Chemical Catalog Company, Inc., 1932.
14. Kassel, L.S., J. Phys. Chem., 32 (1928) 225.
15. Kassel, L.S., J. Phys. Chem., 32 (1928) 1065.
16. Kassel, L.S., Proc. Natl. Acad. Sci. USA, 14 (1928) 23.
17. Glasstone, S. et al., The Theory of Rate Processes, McGraw-Hill Book Co., New York, NY, 1941.
18. Present, R.D., Kinetic Theory of Gases, McGraw-Hill Book Co., 1958.
19. Vicanek, M. and Ghoniem, N.M., J. Comp. Phys., 100 (1992) 1.
20. Stone, C.A., Vicanck, M. and Ghoniem, N.M., J. Comp. Phys., 104 (1993) 451.
21. Lowe, J.P., Quantum Chemistry, 2nd ed., Academic Press, New York, NY, 1993.
22. Park, D.A., Introduction to the Quantum Theory, McGraw-Hill Book Co., New York, NY, 1964.
23. Schmidt, M.W. et al., J. Comput. Chem., 14 (1993) 1347.

24. McLeanand, A.D. and Chandler, G.S., J. Chem. Phys., 72 (1980 (5639).
25. Stewart, J.J.P., J. Comput. Chem., 10 (1989) 209.
26. Gardiner Jr., W.C. and Troe, J., In Gardiner Jr., W.C. (Ed.) Combustion Chemistry, Springer-Verlag, New York, NY, 1984, pp. 173–196.
27. Weast, R.C., CRC Handbook of Chemistry and Physics, 61st ed., CRC Press, Cleveland, OH, 1981.
28. Perry, R.H. and Chilton, C.H., Chemical Engineers' Handbook, 5th ed., McGraw-Hill Book Co., 1973.
29. Radhakrishnan, K. and Hindmarsh, A.C., Description and Use of LSODE, the Livermore Solver for Ordinary Differential Equations, Lawrence Livermore National Laboratory Report UCRL-ID-113855, NASA Reference Publication 1327, 1993.
30. Atkins, P.W., Molecular Quantum Mechanics, Oxford University Press, Oxford, 1986.
31. Pople, J.A. and Beveridge, D., Approximate Molecular Orbital Theory, McGraw-Hill Book Co., 1970.
32. Olander, D.R., Fundamental Aspects of Nuclear Reactor Fuel Elements, 39–40, Technical Information Center, Energy Research and Development Administration, 1976.
33. Tersoff, J., Phys. Rev. Lett., 61 (1988) 2879.
34. Rao, N. et al., J. Mater. Res., 10 (1995) 2073.
35. Rao, N., Girshick, S., Heberlein, J., McMurry, P., Jones, S., Hansen, D. and Micheel, B., Plasma Chem. Plasma Processing, 15 (1995) 581.